Wang, Peng et al.

Article

Stochastic management of hybrid AC/DC microgrids considering electric vehicles charging demands

Energy Reports

Provided in Cooperation with:
Elsevier

Suggested Citation: Wang, Peng et al. (2020) : Stochastic management of hybrid AC/DC microgrids considering electric vehicles charging demands, Energy Reports, ISSN 2352-4847, Elsevier, Amsterdam, Vol. 6, pp. 1338-1352, https://doi.org/10.1016/j.egyr.2020.05.019

This Version is available at:
https://hdl.handle.net/10419/244125

Energy Reports 6 (2020) 1338–1352

Contents lists available at ScienceDirect

Energy Reports

journal homepage: www.elsevier.com/locate/egyr

Research paper

Stochastic management of hybrid AC/DC microgrids considering electric vehicles charging demands

Peng Wang [a], Dan Wang [b], Chengliang Zhu [b], Yan Yang [c], Heba M. Abdullah [d], Mohamed A. Mohamed [e,f,*]

[a] State Grid Hubei Electric Power Co., Ltd., Wuhan, Hubei 430077, China
[b] Jiaxing Power Supply Company of State Grid Zhejiang Electric Power Co., Ltd., Jiaxing, Zhejiang 314000, China
[c] Tus-Institute for Renewable Energy, Qinghai University, Xining, Qinghai 810016, China
[d] Electrical Engineering Department, College of Engineering, Qatar University, Doha 2713, Qatar
[e] Department of Electrical Engineering, Fuzhou University, Fuzhou 350116, China
[f] Electrical Engineering Department, Faculty of Engineering, Minia University, Minia 61519, Egypt

ARTICLE INFO

Article history:
Received 7 April 2020
Received in revised form 4 May 2020
Accepted 20 May 2020
Available online xxxx

Keywords:
Hybrid AC/DC microgrids
Uncertainty
Electric vehicles
Optimization
Charging patterns
Flower pollination algorithm

ABSTRACT

The high growth of the automotive industry reveals the very bright future of this technology and its high penetration effects on the human society. No doubt that the random and volatile charging demand of these devices would affect the power grid optimal operation and scheduling which may be regarded as a new challenge. Therefore, this paper investigates the stochastic scheduling of hybrid AC/DC microgrids considering the plugin hybrid electric vehicles charging demands, distributed all over the grid. Three different charging patterns, called coordinated, uncoordinated and smart charging models with different characteristics for the charger type, capacity and market share are proposed. Moreover, different types of renewable energy sources including wind turbine, solar panel and fuel cell are modeled and considered in the scheduling process of the hybrid microgrid. In order to mitigate the charging effects of electric vehicles on the hybrid AC–DC microgrid operation, some remotely switches are considered in the system which make it possible for changing the topology and power flow way. In order to model the uncertainty effects, a data-driven framework based on point estimate method and support vector machine is developed. This would make it possible to extract out the standard deviation value of the uncertain parameters and reflect their impacts on the microgrid operation problem through the limited concentration points. A novel evolving solution based on flower pollination algorithm is also proposed to solve the problem optimally. An IEEE standard test system is used as the hybrid AC/DC microgrid case study to assess the performance of proposed model.

1. Introduction

Opportunities and openings provided by the hybrid AC/DC microgrids support the concept of both AC and DC technologies in distributed generations (DGs) without any need to the converters. Harvesting energy directly from varied types of renewable energy sources such as solar units with DC power, fuel cells with DC power and wind turbine with AC power as well as the dispatchable units like microturbines make a great opportunity for high power quality and reliability of the system but with low capital cost. Compared to the just-AC microgrids or just-DC microgrids, the hybrid AC/DC microgrids bring some new advantages such as lower investment costs, omitting converters, higher power quality and direct power supply at the location (Naderi et al., 2017; Aghajani and Ghadimi, 2018; Aprilia et al., 2019). Therefore, it is quite expected that the future market would see high growth of this technology with different types of DGs. Still it is quite agreed among researchers (Gong et al., 2020; Wang et al., 2014) that this will bring new challenges to how one can manage the high penetration of renewable energy sources along the optimal operation and management of these grids. In addition, the entrance of electric vehicles as new loads in the grid will add up to the complexity of this issue by asking electrical charging demands at a random nature all over the grid. In this situation, the coordination among the electric vehicles, renewable sources and the hybrid microgrid is a key subject, which needs further assessment. In recent years, some surveys have been implemented to answer parts of these question which some of the most significant ones are provided in the rest.

* Corresponding author at: Electrical Engineering Department, Faculty of Engineering, Minia University, Minia 61519, Egypt.
E-mail address: dr.mohamed.abdelaziz@mu.edu.eg (M.A. Mohamed).

https://doi.org/10.1016/j.egyr.2020.05.019

Nomenclature

Constants

B_{Gi}^t	Price of the generator offer
B_{sj}^t	Price of the storage offer
${B_{Grid}}^t$	Price of the main utility
c_1, c_2	Charging starting time characteristics in different schemes.
C_{bat}	Battery capacity
P	Charger rating
σ, μ	Variance and average value of the normal probability function of smart charging
η	Charger efficiency
$\mu_{c\rho}$	Average value of the uncertain parameter
ρ	Number of uncertain parameters
ω	Weighting factor value for point estimate method
$\overline{C_{bat}}/\underline{C_{bat}}$	Upper/lower bound on the battery capacity
$\mu_{C_{bat}}/\sigma_{C_{bat}}$	Parameters of battery capacity
N	Number of data samples in prediction model
ε	A constant value showing the margins in support vector
C	Balancing constant parameter between training error and structure complexity
$\xi_{l,k}$	Standard location parameter
N_T/N_g	Number of time intervals/number of generators
S_{Gi}^{on}/S_{Gi}^{off}	Price of ON/Off switching of generators
N_{RCS}	Number of remotely switches
N_{Load}	Number of load levels
λ_{RCS}	Price of switching due to aging
$P_{Load,k}^t$	Amount load level k
N_b	Number of buses
M_{tie}	Number of tie switches of grid.
M_{Sw}	Number of sectionalizing switches of grid.
$S_i^{Line,t}/S_{i,\max}^{Line}$	Amount/maximum of apparent power flowing on the lines between buses b and k
${p_{Gi,\max}}^t/{p_{Gi,\min}}^t$	Maximum/minimum technical limit of the generator
${p_{sj,\min}}^t/{p_{sj,\max}}^t$	Maximum/minimum technical limit of the storage unit
${p_{grid,\min}}^t/{p_{grid,\max}}^t$	Maximum/minimum technical limit of the main grid
$\eta_{charge}/\eta_{discharge}$	Efficiency of charging/discharging
$W_{ess,\max}/W_{ess,\min}$	Maximum/minimum limit of energy storage of the battery
$P_{charge,\max}$ $/P_{discharge,\max}$	Maximum charging/discharging capacity
NL	Number of lines
∇	Balancing variable between the abiotic and abiotic search in MFPA
Δ	Constant parameter on FPA

Variables

t_{start}	Charging starting time for electric vehicle
f	Objective function
m	Driving mileage
ζ	All electric range
SoC	Battery state of the charge of battery electric vehicle
DoD	Depth of Discharge in electric vehicle
t_D	Charging duration
x, y	Input and output samples to the prediction model
W/b	Weighting and biasing coefficients of support vector machine
$\varphi(x)$	Nonlinear function of support vectors
Θ_ε	Loss function in support vector machine
ξ^*, ξ	Upper and lower training error
β_t^*/β_t	Dual variables of the support vector optimization
$\Omega(x_t, x)$	Kernel function
σ_c	Standard deviation of the RBF kernel function
z_l	lth uncertain parameter
$\Upsilon_{l,3}$	Skewness coefficient
f_l	Cost function value of lth solution
S_i	Output function value
${u_i}^t$	On/off status of generators
p_{sj}^t	Output power of storage
${p_{Grid}}^t$	Out power of the main grid
$N_{RCS,i}^{Sw}$	Number of switching operations
$P_m^{Inj,t}/Q_m^{Inj,t}$	Net injected active/reactive power
W_{ess}^t	Amount of energy stored in the battery storage
$P_{charge}/P_{discharge}$	Amount of charging/discharging power of battery
w_{it}	Status of ith feeder at time t
λ_{Tie}, λ_{Sw}	ON/ODD status of tie and sectionalizing switches
μ_y/C_y	Average/standard deviation of the output function
X_l^k	Control vector (pollen in FP) in iteration k
χ	Random variables in the range (0,1]
r_l	Random value in the range (0,1]
${V_m}^t/{\delta_m}^t$	Voltage magnitude/phase of bus m at hour t.
Y_{mk}/θ_{mk}	Magnitude/phase of impedance between bus m and k.
τ	Random value between $[-1,1]$.

In Esfahani and Mohammed (2019), a categorized routing approach is used for the real-time operation of unbalanced hybrid microgrids with electric vehicles. In that model, charging stations with dynamic routing are also considered in the analysis to minimize the power losses and enhance the imbalance factor. The simulation results on the IEEE 13 bus show the improved loadability of the hybrid microgrid. In Amirkhan et al. (2020), a robust method is proposed to control a hybrid AC/DC microgrid

considering load-varying characteristics. The passivity theory is deployed for returning all-state variables to the stable operation point and proving precise power sharing among units. In Sur et al. (2020), a new load flow approach based on holomorphic theory is suggested for the operation of hybrid AC/DC microgrids. The power flow equations are then solved by Pade approximant using the feeder impedance values. The simulation results show the robustness and efficiency of the proposed load flow method. In Eghtedarpour and Farjah (2014), hybrid microgrid technology is proposed as a supportive idea for interconnection of DGs compared to AC microgrids and DC microgrids. To this end, an interconnection converter is designed to control and operate the microgrid in the grid connected and islanded modes of operation. To minimize the number of communicating links among the generators and the microgrid, a decentralized solution is proposed for this target. Authors in Dabbaghjamanesh et al. (2020) focus on the optimal scheduling of reconfigurable AC–DC microgrids considering dynamic line rating. The proposed method considers the environmental factors such as solar radiation, wind speed and temperature to amend the power flow equations. In addition, a new linear optimization method is devised to relax the problem nonlinearities. In Balderrama et al. (2019), a hybrid AC/DC microgrid is designed for the robust electrifying of a remote rural area in Bolivia considering the uncertainty effects. The model uses the long-term historical data to run a stochastic mixed integer linear programming model. In Ayodele et al. (2019), an energy management method is proposed for a hybrid AC/DC microgrid in the rural residential locations. The model considers wind turbine, solar panels, gasoline and battery to provide high reliability for continued power supply. Energy resource availability analyses show the capability of the microgrid for not only supplying the electrical demands but also for charging some excess devises such as water pumping machine and rural home lighting. In Ray and Mohanty (2019), a hybrid firefly and particle swarm optimization approach is proposed to regulate the frequency of a hybrid AC–DC microgrid in the presence of wind, solar units, fuel cell, storages and engine generators. A PID controller is also deployed for minimizing the frequency variations when load experiences high changes. Authors in Ge et al. (2020) suggest a distributed control mechanism for hybrid microgrids to assess the stability of the system and provide a proper power sharing. The stability of the system is assessed through the modeling and eigenvalue extraction of the model for the first time. A complete survey on the fundamentals of the hybrid AC/DC microgrids is provided in Pourbehzadi et al. (2019). Also, a valid comparison among different renewables, optimization methods and control zones is provided.

As it can be concluded from the above explanations, the idea of hybrid AC/DC microgrids has become the center of attention of many researchers in recent years (Mohamed et al., 2020b; Tabar et al., 2019). This is not only because of the new type of technology which is offered here but rather because of its many benefits coming from the encompassing AC and DC structures. Therefore, this paper aims to investigate the optimal operation and management of renewable based hybrid AC/DC microgrids in the presence of electric vehicles. This is a challenging task due to the random and complex nature of the charging demand of the electric vehicles distributed in the grid. Owing to the high popularity, plug in hybrid electric vehicles are modeled and analyzed with different penetration levels of 40% and 80% all over the hybrid AC/DC microgrid. Four different charging types with a varied market share and capacity are also considered to enrich the analysis (Guo et al., 2019). In order to mitigate the negative effects of the electric vehicles charging demand on the grid, the idea of optimal switching is developed which will alter the power flow paths through feeder reconfiguration. This also provided a better matching among the renewable energy sources and the dispatchable units to release their capacities. A stochastic framework based on point estimate method is proposed to handle the high randomness caused by the renewable energy sources of solar and wind as well as the charging demand of the plug in hybrid electric vehicles in the system. A machine learning approach based on support vectors (Shao et al., 2020) is also proposed to estimate the standard deviation parameters in the wind and solar data forecast error. This would help to have a more precise uncertainty modeling procedure. Support vector machine keeps a hyper plane on the training error to avoid the high structural complexity. The objective function is the total cost of the hybrid microgrid for electrifying the loads and electric vehicles and the switching costs due to the aging issues. Because of the high nonlinearity and complexity of the optimization problem, a novel optimization method based on flower pollination algorithm (Peesapati et al., 2018) is proposed. It is a well-perceived concept in the literature that the discrete optimization problems belong to the category of hard optimizations, which need powerful optimizers (Vasant et al., 2019a,b). Therefore, it is always needed to find a way for adopting the optimization method with the problem nature. Fuzzy based modification (Ganesan et al., 2020), machine learning (Al-Saud et al., 2020) and math-based operators (Mohamed et al., 2020a) are along the well-known approaches proposed in the literature. Therefore, a novel dynamic modification method is presented in this paper to increase the pollen diversity and avoid possible premature convergence. Therefore, the main contributions of this research work can be summarized as follows:

- Modeling and investigating the charging effect of plug in hybrid electric vehicles on the optimal operation of hybrid microgrids for different charger types, market share, vehicle type, etc.
- Proposing a novel data driven stochastic framework based on point estimate method and support vector machine for modeling the uncertainties of the renewables, loads and charging demands of electric vehicles, precisely
- Deploying the optimal switching strategy for mitigating the random charging effects of the plug in hybrid electric vehicles on the AC/DC microgrids operation problem
- Assessing different charging schemes with varied charger types and market share for the plug in electric vehicles
- Proposing an effective modified optimization method based on flower pollination algorithm to solve the energy management problem in the hybrid AC/DC microgrids

The high capability and feasibility of the proposed stochastic model is assessed on an IEEE test system. The rest of this paper is organized as follows: Section 2 explains the electric vehicle charging modeling, technology and characteristics. Section 3 describes the proposed data-driven stochastic framework based on point estimate method and support vector machine to handle the uncertainty effects. The problem formulation for energy management of the hybrid AC/DC microgrid is provided in Section 4. Section 5 is devoted to the solution procedure and how to solve the problem. In Section 6, the simulation results on the IEEE test system are investigated to assess the proposed model performance. Finally, the main outcomes and results are concluded in Section 7.

2. Plug in hybrid electric vehicle and charging schemes

The recent growth of vehicle market shows high demands for more energy saving and cleaner productions to avoid the world global warming and provide more economic systems. Although the pure electric vehicles can help to achieve this goal, but the high battery price and short driving mileage are some of the main

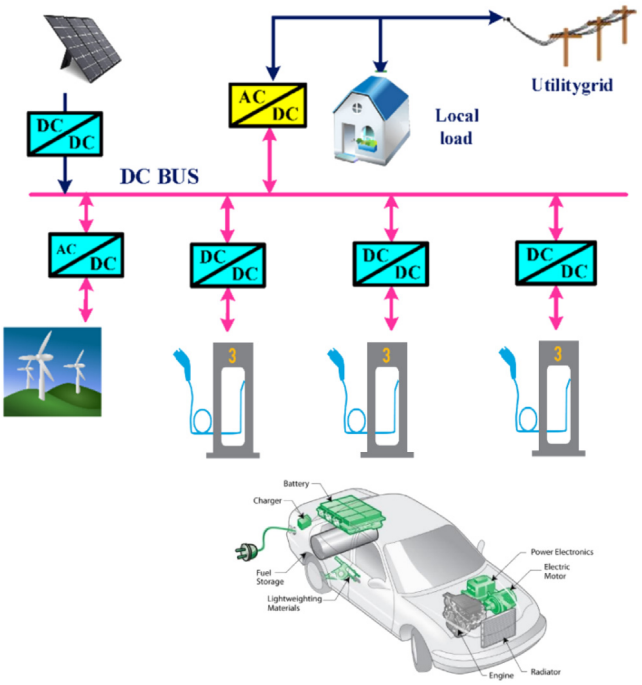

Fig. 1. Plug in hybrid electric vehicles as new electrical loads in the microgrids.

barriers in front of this technology. Therefore, a transitioning technology from the fossil fuel based vehicles to pure electric vehicles can be the plug-in hybrid electric vehicle with lower cost and higher driving mileage. From the power utility point of view, this is but a new electric load consumer with highly complex and random charging behavior, which can cause new challenges in the optimal operation and management of the power systems. Therefore, it is critical for the power grids, specially the microgrids, to model this charging demand in a practical and useful realistic way. In order to model the charging demand of plug in hybrid electric vehicles, some parameters such as number of vehicles in the charging mode, the charger type (rate and capacity), state of charge (SoC), charging time and length of being in the charging mode are significant. Most of these factors are still uncertain which can cause the entire behavior of the electric vehicle to be uncertain from the power grid point of view. In this section, three different charging schemes, called coordinated, uncoordinated and smart charging, are introduced to model the charging demand of plug in hybrid electric vehicles in the hybrid AC/DC microgrids (see Fig. 1).

Uncoordinated Charging: In this charging model, it is assumed that the car will plug into the charger at any time in the day. As a normal daily life pattern, people (and thus the vehicle) leave the home at the early morning and return home in the evening. In this situation, the majority of vehicles start charging around 6 pm, when the driver gets home. This makes us to consider a uniformly distributed probability density function with an effective domain around 6 pm for the charging starting time. The mathematical representation of this idea can be shown as below (Li and Zhang, 2012):

$$f(t_{start}) = \frac{1}{c_1 - c_2} \quad c_1 \le t_{start} \le c_2 \quad c_1 = 18, c_2 = 19 \tag{1}$$

Coordinated Charging: In this charging pattern, the vehicle owner has a tendency to charge his/her car at light-load hours, to avoid concurring the evening peak load hours. This will bring economic savings to the car owner due to lower billing prices. Therefore, the driver decides to postpone the charging time to any time after 9 pm. This charging pattern is interpreted in such a mathematical formulation:

$$f(t_{start}) = \frac{1}{c_1 - c_2} \quad c_1 \le t_{start} \le c_2 \quad c_1 = 21, c_2 = 24 \tag{2}$$

Smart Charging: In the last charging model, the vehicle charging happens in the most favorable way, which means at hours that electricity price is low, demand is not high and there is adequate capacity in the grid. Such an attractive charging pattern can benefit both the driver and the utility both technically and economically. Considering the complex characteristics of this charging pattern, a normal probability density function is considered for this case:

$$f(t_{start}) = \frac{1}{\sigma\sqrt{2\pi}} e^{(-\frac{1}{2}(\frac{t_{start}-\mu}{\sigma})^2)} \quad \mu = 1, \sigma = 3 \tag{3}$$

When the vehicle plugs into the charging socket, it initiates the charging process. The battery SoC can be further calculated according to the driving distance of the vehicle. The normal daily driving distance for a vehicle is reported to follow a log-normal probability density function as below (Li and Zhang, 2012):

$$f(m) = \frac{1}{m\sigma\sqrt{2\pi}} e^{\frac{-(\ln(m)-\mu)^2}{2\sigma^2}} \quad m > 0 \tag{4}$$

The amount of the battery SoC at the moment of plugging into the charger can be calculated based on its driving distance and all electric range (ζ) as below:

$$SoC = \begin{cases} 0 & m > \xi \\ \dfrac{\xi - m}{\xi} \times 100\% & m \le \xi \end{cases} \tag{5}$$

In the market, there are varied types of plug in hybrid electric vehicles such as EV-20, EV-30, EV40 and EV-60, wherein the number represents ζ. According to the high popularity in the market, EV-20 is chosen to be studied in this research. Other types can be used with the same procedure. Having this, the charging length can be evaluated based on SoC as below (Li and Zhang, 2012):

$$t_D = \frac{C_{bat} \times (1 - SOC) \times DOD}{\eta \times P} \tag{6}$$

It was mentioned previously that an electric vehicle starts charging when it gets home depending on its electrical charging demands. Also, it is recommended that the battery depth of discharge (DoD) does not exceed a specific value (noted as 80% Avatefipour et al., 2019) to avoid fast aging process. According to (6), the charging length depends on the charger efficiency and rate parameters. Table 1 provides the electric vehicle charger characteristics based on the type, voltage level and the capacity. In this table, type 1 and 2 are the home chargers and type 3 is a public charger. The option that determines the success of an electric vehicle in the automotive market (market share) is the battery technology. Thus, Table 2 shows four-battery technology in the electric vehicle work.

Due to the fact that market share follows a discrete distribution, the type of the vehicle is randomly chosen based on the

Table 1
Chargers characteristics for plug in hybrid electric vehicles.

Charger type	Nominal voltage	Power capacity (kW)
Level 1	120 VAC	1.44
Level 2	208–240 VAC	11.5
Level 3	208–240 VAC	96
Level 3 (DC)	208–600 VDC	240

Table 2
Types of plug in hybrid electric vehicles with market share (Avatefipour et al., 2019).

Type	Market share	Min capacity (C_{bat}) in kWh	Max Capacity C_{bat} in kWh
Micro Car	0.2	8	12
Economy Car	0.3	10	14
Mid-Size Car	0.3	14	18
Light Truck/SUV	0.3	19	23

market share. This would be made possible by using the roulette wheel mechanism (Roustaei et al., 0000) in this paper. The capacity of the vehicle battery C_{bat} belonging to each type in Table 2 follows a normal distribution function with these parameters (Li and Zhang, 2012):

$$\mu_{C_{bat}} = \frac{\underline{C_{bat}} + \overline{C_{bat}}}{2}$$
$$\sigma_{C_{bat}} = \frac{\underline{C_{bat}} - \overline{C_{bat}}}{4} \tag{7}$$

3. Data-driven stochastic framework

In order to model the uncertainties of the problem, a novel data-driven approach based on point estimate method and advanced machine learning is proposed. In the first stage, support vector machine is deployed as the predictor to find out the standard deviation of the forecast error for each uncertain parameter according to its historical data. These data are then used in the point estimate method for mapping the input uncertainty on the output. These methods are explained in the rest.

3.1. Support vector machine

Support vector machine is an advanced machine learning approach which belongs to the supervised learning category. In contradiction of the artificial neural network (ANN) which may encounter overfitting issues, support vector machine creates a hyper plane to keep the network structure complexity when minimizing the training error. It is claimed in support vector theory (Shao et al., 2020) that it is possible to find a linear relationship for any nonlinear mapping but in a higher dimension. Let us start with the input dataset $\{(x_i, y_i)\}^N$ in the space $\Re^n$. The mapping to a higher dimension space $\varphi(.): \Re^n \rightarrow \Re^{n_h}$ would provide a linear function f representing the relationship between x_i and y_i as follows:

$$f(x) = W^T\varphi(x) + b \tag{8}$$

The weighting factor and biasing factor W and b can be evaluated by solving the following equations (Shao et al., 2020):

$$\text{Min } R_{SVR} = \frac{1}{N}\sum_{t=1}^{N} \Theta_\varepsilon(y_t, W^T\varphi(x_t) + b) \tag{9}$$

$$\Theta_\varepsilon(y, f(x)) = \begin{cases} |f(x) - y| - \varepsilon \; ; & |f(x) - y| \geq \varepsilon \\ 0 \; ; & \text{Otherwise} \end{cases} \tag{10}$$

$\Theta_\varepsilon(y, f(x))$ is the loss function for penalizing the very wide support vectors. In order to construct the model, support vector machine not only does minimize the training error, but also keeps a hyper plane on the model complexity, concurrently. This combinatorial idea is shown as below:

$$Min_{W,b,\xi^*,\xi} R_\varepsilon(W, \xi^*, \xi) = \frac{1}{2}W^TW + C\sum_{t=1}^{N}(\xi_i^* + \xi_i) \tag{11}$$

In (11), the first term reflects the model complexity and the second term reflects the training error. Fig. 2 depicts the support vector machine idea when making the nonlinear transition from the initial space to the higher dimension. In this figure, ξ_i displays the training error below $-\varepsilon$ and ξ_i^* displays the training error above $+\varepsilon$.

The above problem is then reformulated in a limited shape as follows:

$$\begin{aligned} &y_t - W^T\varphi(x_t) - b \leq \varepsilon + \xi_t^* \quad ; \quad t = 1, \ldots, N \\ &-y_t + W^T\varphi(x_t) + b \leq \varepsilon + \xi_t \; ; \quad t = 1, \ldots, N \\ &\xi_t^* \geq 0 \, ; \, \xi_t \geq 0 \qquad\qquad ; \quad t = 1, \ldots, N \end{aligned} \tag{12}$$

The feasible solution of the above problem would result in the optimal value of W as follows (Kavousi-Fard et al., 0000):

$$W = \sum_{t=1}^{N}(\beta_t^* - \beta_t)\varphi(x_t) \tag{13}$$

Therefore, (5) can then be reshaped based on the optimal value of W as below:

$$f(x) = \sum_{i=1}^{N}(\chi_t^* - \chi_t)\Omega(x_t, x) + b$$
$$\Omega(x_t, x) = \varphi(x_t) \circ \varphi(x_t) \tag{14}$$

It should be noted that $\Omega(x_t, x)$ is called a kernel function. In the mathematic definition, a function is called a kernel type if it satisfies the Mercer's condition (Kavousi-Fard et al., 0000). Among different kinds of kernel functions, we use the radial basis function due to its smooth shape, high nonlinearity modeling capability and simple idea:

$$K(x_t, x_j) = \exp(-0.5 \left\| x_t - x_j \right\|^2 / {\sigma_c}^2) \tag{15}$$

3.2. Point estimate method

For modeling the uncertainty impacts on the optimal energy management of the hybrid AC/DC microgrids, point estimate method gives a very proper solution for finding the precise result with much less computational effort compared to the Monte Carlo simulation. Assuming ρ number of uncertain parameters, point estimate method generates $2\rho + 1$ deterministic frameworks to handle the uncertainty effects. Requiring very few statistical features of the uncertain parameter, low computational burden and compatibility with both discrete and continuous optimization problem are the main features of point estimate method. In order to explain this method, Fig. 3 shows the conceptual concept of point estimate method. According to this figure, a nonlinear mapping between the input and output space of the problem can be provided through the limited number of points matching the probability density function of the uncertain parameter.

Let us show the nonlinear power flow equations by F, the input uncertain vector z (wind turbine, solar panel, load demand, market price, charging characteristics of the electric vehicles) and the output vector S (power losses and cost function) in this form:

$$S = F(z) \tag{16}$$

As it is perceived from the above equation, the input uncertainty would move to the output through the nonlinear function F. Let us suppose that the input uncertain parameter z_l has the probability density function of U_{zl}. Point estimate method replaces each U_{zl} by two concentration points $z_{l,k}$ ($1 = 1,2$) by fitting its average, variance and skewness coefficient (Kavousi-Fard and Niknam,

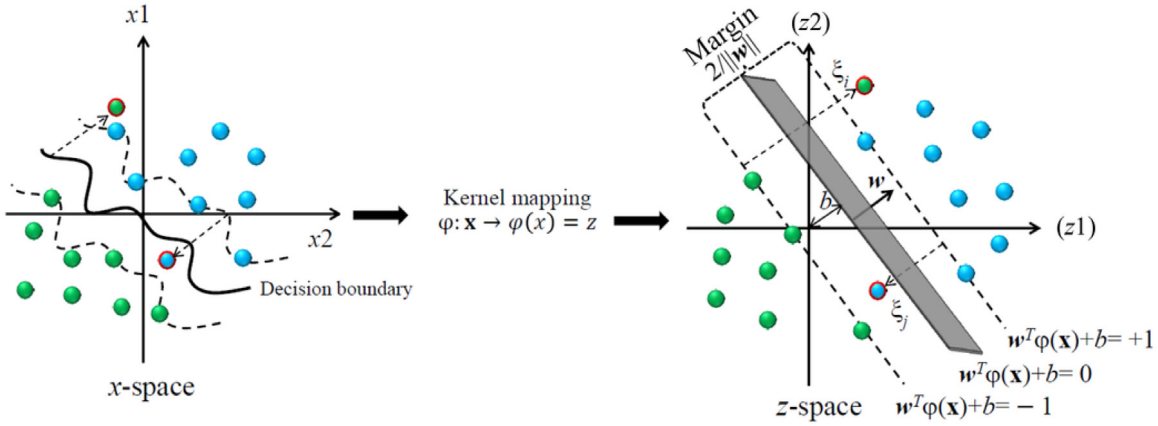

Fig. 2. The core idea of support vector machine for nonlinear mapping.

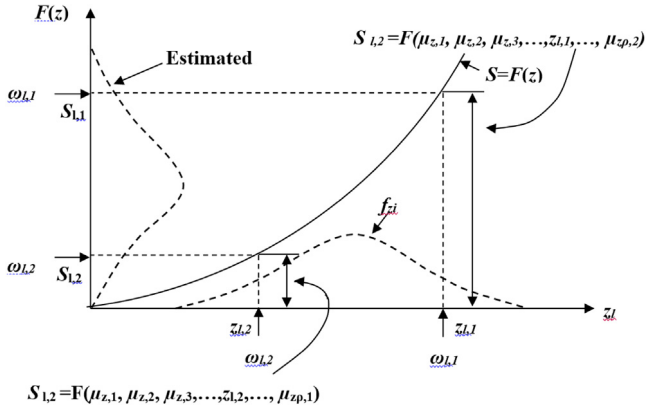

Fig. 3. The concept of nonlinear mapping of point estimate method.

2015). Considering μ_z as the average of the uncertain parameter, the method creates 2ρ deterministic frameworks as follows:

$$S = F(\mu_{z1}, \mu_{z2}, \ldots, z_{l,k}, \ldots, \mu_{z\rho}); k = 1, 2 \tag{17}$$

Each concentration point is then computed for the input uncertain parameter z_l as follows:

$$z_{l,k} = \mu_{z_l} + \xi_{l,k}.\sigma_{z_l}; \quad k{=}1, 2 \tag{18}$$

The standard location parameter can be evaluated as:

$$\xi_{l,k} = \frac{\Upsilon_{l,3}}{2} + (-1)^{3-k}\sqrt{\rho - (\Upsilon_{l,3}^2/2)^2}, \quad k = 1, 2 \tag{19}$$

The skewness coefficient ($\Upsilon_{l,3}$) as the third moment can be computed as:

$$\Upsilon_{l,3} = \frac{E\left[\left(z_l - \mu_{z_l}\right)^3\right]}{\left(\sigma_{z_l}\right)^3} \tag{20}$$

The impact of each point $z_{l,1}$ and $z_{l,2}$ on the output cost function is shown by the weighting factors $\omega_{l,1}$ and $\omega_{l,2}$, respectively. After calculating (17) for 2ρ times, the expected value and the standard deviation S_i can be evaluated (Kavousi-Fard and Niknam, 2015):

$$\begin{aligned} &\sigma = \sqrt{\text{var}(S_i)} = \sqrt{E(S_i^2) - [E(S_i)]^2} \\ &E(S_i^j) = \sum_{l=1}^{\rho}\sum_{k=1}^{2}(\omega_{l,k} \times S_i^j(\mu_{z1}, \mu_{z2}, \ldots, z_{l,k}, \ldots, \mu_{z\rho})) \\ &\omega_{l,k} = \frac{1}{2\rho} \end{aligned} \tag{21}$$

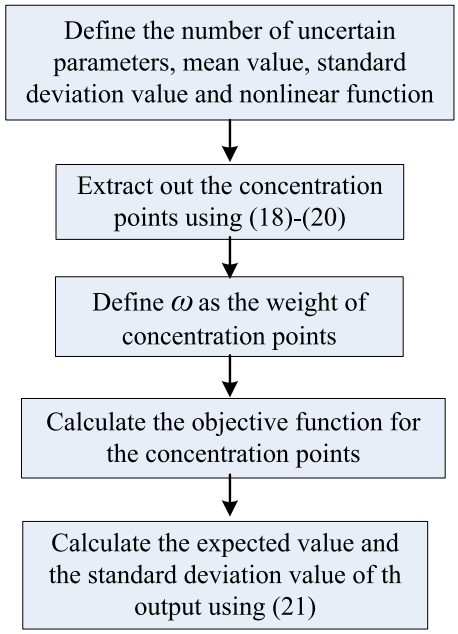

Fig. 4. Flowchart of the point estimate method.

Fig. 4 shows the flowchart of the point estimate method.

4. Energy management problem formulation

This section explains the problem formulation including the cost function and the relevant constraints. The cost function consists of several terms: (1) cost of power purchased from DGs, (2) cost of power purchased from the storage unit, (3) cost of start-up and shut-down of units and (4) cost of power purchased from the power utility and (5) cost of switching as follows:

$$\begin{aligned} Min \quad E(Cost) = &\sum_{t=1}^{N_T}\sum_{i=1}^{N_g}[u_i{}^t E(p_{Gi}^t)B_{Gi}^t + S_{Gi}^{on}\max\{0, u_i{}^t - u_i^{t-1}\} \\ &+S_{Gi}^{off}\max\{0, u_i{}^{t-1} - u_i{}^t\}] \\ &+\sum_{j=1}^{N_s}[u_j{}^t E(p_{sj}^t)B_{sj}^t] + E(p_{Grid}{}^t)B_{Grid}{}^t + \sum_{i=1}^{N_{RCS}} N_{RCS,i}^{sw}\lambda_{RCS} \end{aligned} \tag{22}$$

The cost function is optimized by meeting several operation constraints as follows:

– *Generation and Demand Balance in DC and AC areas*: In both AC and DC areas of the microgrid, the balance between the demand and generation should be preserved. In the DC area, this can be achieved by:

$$\sum_{i=1}^{N_g} E(p_{Gi}^t) + \sum_{j=1}^{Ns} E(p_{sj}^t) + E(p_{Grid}^t) = \sum_{k=1}^{N_{Load}} E(P_{Load,k}^t) \tag{23}$$

For the AC area, the generation and demand balance is preserved by running the power flow:

$$E(P_m^{Inj,t}) = \sum_{n=1}^{N_B} E(V_m^t)E(V_n^t)Y_{mn}\cos\left(\Theta_{mn} + E(\delta_m^t) - E(\delta_n^t)\right) \tag{24}$$

$$E(Q_m^{Inj,t}) = \sum_{n=1}^{N_B} E(V_m^t)E(V_n^t)Y_{mn}\sin\left(\Theta_{mn} + E(\delta_m^t) - E(\delta_n^t)\right) \tag{25}$$

– *Generation Capacity*: Technically, each power source, either DG, storage unit or the main grid, has a maximum and minimum capacity which is modeled as a constraint:

$$\begin{aligned} &{p_{Gi,\min}}^t \le E({p_{Gi}}^t) \le {p_{Gi,\max}}^t \\ &{p_{sj,\min}}^t \le E({p_{sj}}^t) \le {p_{sj,\max}}^t \\ &{p_{grid,\min}}^t \le E({p_{Grid}}^t) \le {p_{grid,\max}}^t \end{aligned} \tag{26}$$

– *Storage Capacity*: The storage unit can charge/discharge in a limited range with respect to its maximum capacity as below:

$$E(W_{ess}^t) = E(W_{ess}^{t-1}) + \eta_{charge}E(P_{charge})\Delta t - \frac{1}{\eta_{discharge}}E(P_{\text{discharge}})\Delta t$$

$$\begin{cases} W_{ess,\min} \le E(W_{ess}^t) \le W_{ess,\max} \\ E(P_{charge,t}) \le P_{charge,\max} \\ E(P_{discharge,t}) \le P_{discharge,\max} \end{cases} \tag{27}$$

– *Feeder Thermal Limit*: The feeders have specific thermal limits which are modeled in the problem as follows:

$$|E(S_i^{Line,t})| < S_{i,\max}^{Line} \tag{28}$$

– *Bus Voltage Limit*: Any bus in the microgrid can tolerate a maximum and minimum voltage level as below:

$$V_m^{\min} \le E(V_m^t) \le V_m^{\max} \tag{29}$$

– *Keeping the radiality*: From the protection point of view, it is much simpler to keep the system radial for the coordination of overcurrent relays. When switching, it is possible to alter the feeder power flow path. This might cause a loop in the system which can be removed quickly to keep the system radial. The number of loops in a graph (microgrid topology) with *NL* lines is calculated as follows:

$$\sum_{q\in Q} w_{it} = NL_q - 1 \tag{30}$$

where w displays the status of ith feeder at time t. If $w = 1$, then the line is in service and if $w = 0$ it is out of service.

5. Modified flower pollination algorithm

From the previous section, it is deduced that the front optimization problem is a nonlinear and discrete one which requires an organized optimization method for getting to the global operating point. To this end, we propose an intelligent optimization method based on flower pollination algorithm (FPA). The reason for choosing this method is the powerful local and global operators, which make it suitable for solving mixed integer nonlinear constraint optimization problems. This algorithm is inspired from the pollination phenomenon in the plants for surviving their species. Inspired from the nature, FPA tries to mimic the way that a flower moves its pollens to another plant. In the case of biotic pollination, the flower makes use of the help of alive individuals like insects to transfer its pollens to other types. In the case abiotic pollination, the fertilization happens through the use of wind or rain as the mediate. Compared with each other, biotic pollination takes a larger portion (around 80 percent) in the nature than the abiotic pollination. The movement of the pollens may also happen either in a crossed or self-pollination manner. In crossed way, pollens move to the stigma of another plant with the same type. When self-pollination happens, pollens move from one stigma to another one in the same plant. Keeping these in the mind, FPA is constructed using four key ideas: (1) biotic pollination using the crossed manner represents a global search operator, (2) abiotic pollination using the self-manner represents a local search operator, (3) the local–global search ratio is determined using a constant value called crossed-self-ratio (∇) and (4) local fertilization is more preferred since it has a higher chance for survival.

In order to start the algorithm, the random pollens' population is initiated in the problem feasible domain. By calculating the fitness function value for all pollens, the member with the least cost value is stored as X_g. Then, the pollen population should improve using the above four rules. The global pollination is constructed based on rule number 1 as below:

$$X_l^{k+1} = X_l^k + \partial \times (X_l^k - X_g^k) \qquad \forall l \in \Omega^{FP} \tag{31}$$

Wherein ∂ obeys a Levy agenda in this way:

$$\partial \approx \frac{\lambda\Gamma(\upsilon)\sin(\pi\upsilon/2)}{\pi}\frac{1}{s^{1+\lambda}} \quad (s > 0) \tag{32}$$

The second operator mimics the second rule as the local search operator as below:

$$X_l^{k+1} = X_l^k + r_1 \times (X_{l1}^k - X_{l2}^k) \qquad \forall l \in \Omega^{FP} \tag{33}$$

As per rule number 3, the trade-off between the local and global mechanisms (31) and (33) is preserved using the balancing parameter ∇.

The FPA has exceptional characteristics, which make it a key method for solving the complex optimization problems. However, the performance of the method can yet improve by some modifications in the structure. This will result in a modified version of the algorithm, which are explained in the rest.

– *Modification number* 1**:** The parameter ∇ is assumed constant in the original FPA. In a normal optimization process, global search is preferred more than the local search at the beginning and local search is preferred more than the global search at the end. Such a condition cannot be achieved by a constant value for ∇. Therefore, we propose a dynamic formulation for this parameter as below:

$$\nabla^{k+1} = \left(\frac{1}{\tau \times l}\right)^{\left(\frac{1}{\tau\times l}\right)}\nabla^k;\ \tau \ge 100 \tag{34}$$

According to (34), the parameter ∇ motivate more global search at the beginning and more local search at the end of the optimization.

– *Modification number* 2**:** The second modification method simulates a crossover mechanism between the best solution X_g and

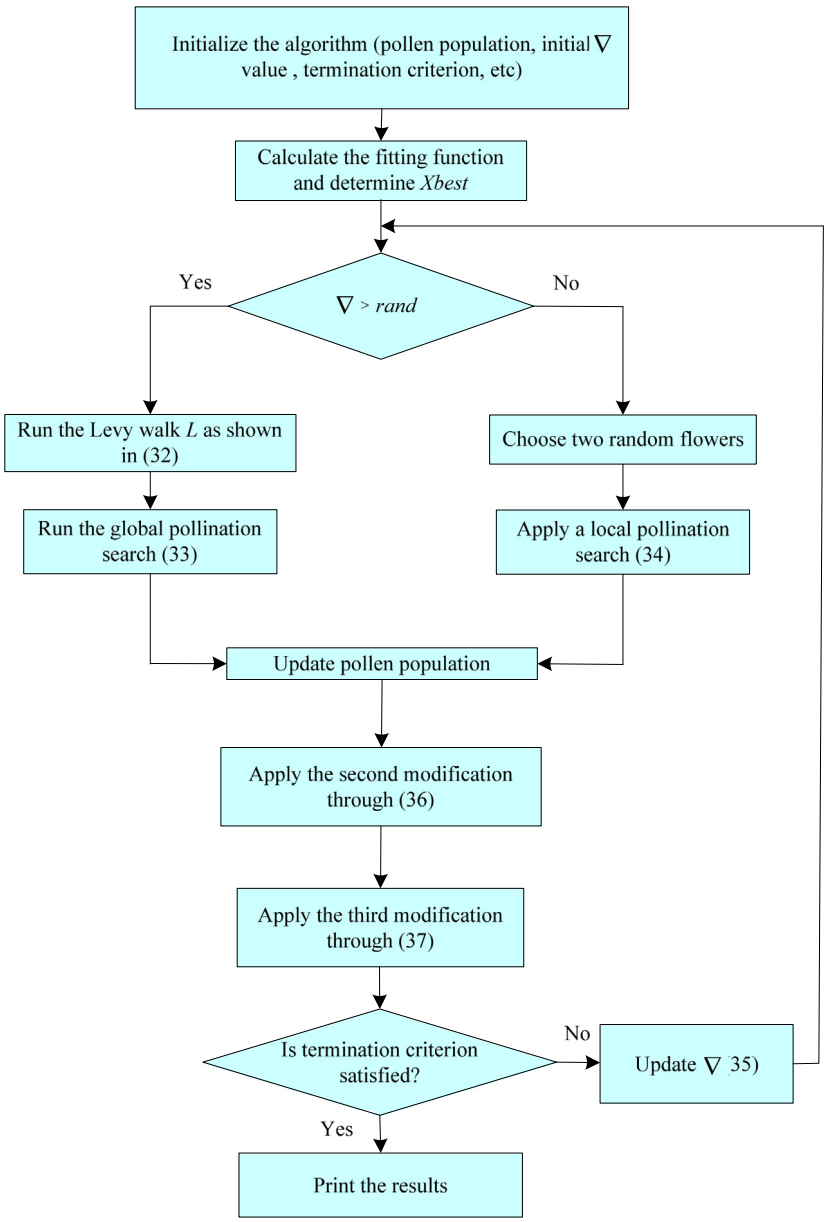

Fig. 5. Flowchart of the MFPA.

each member of the population as follows:

$$\begin{aligned} &if \quad f_{l1} < f_{l2} \\ &X_{Test,i} = X_{l1} + r_2(X_{l1} - X_{l2}) \\ &elseif \quad f_{l2} < f_{l1} \\ &X_{Test,i} = X_{l1} + r_3(X_{l2} - X_{l1}) \\ &End \end{aligned} \tag{35}$$

– *Modification 3*: The third modification improves the pollen population diversity through a fusion approach which let the solutions move to far distances as below:

$$\begin{aligned} &X_l^{k+1} = X_l^k - 0.04[2(1 - \frac{l}{1-k})f_l \frac{\sum_{k=1}^{N_s} \frac{X_k^k}{f_l}}{\sum_{k=1}^{N_s} \frac{1}{f_l}}] + Fus\,(\Delta) \qquad \forall l \in \Omega^k \\ &Fus(\Delta) \approx \frac{\Delta\Gamma(\Delta)\sin(\pi\Delta/2)}{\pi} \frac{1}{s^{1+\Delta}} \quad (s > 0) \end{aligned} \tag{36}$$

The flowchart of the proposed MFPA is shown Fig. 5.

6. Solution procedure

In order to solve the optimal energy management in the hybrid AC/DC microgrids, some steps are needed to run the methods, which were introduced, in the previous sections. These steps are all explained in the rest:

Step 1: Initialize the problem including the hybrid AC/DC microgrid data (bus data, branch data, voltage level, DG locations and capacities, prices, scheduling time horizon, etc.), the optimization MFPA (the size of pollen population, the termination criterion and initial value of ∇), the data-driven stochastic model (the uncertain parameters, recorded data, mean, standard deviation and skewness values of the random parameters), plug in hybrid electric vehicles (charging type, market share, vehicle type, charger rate and capacity, etc.).

Step 2: In order to extract out the standard deviation of the uncertain parameters probability density function, the historical

Table 3
Capacity and bids of the RESs & the utility.

Type		Min power (kW)	Max power (kW)	Bid (€ct/kWh)	Start-up/Shut-down cost (€ct)
Solar panel	1	0	500	2.584	0
Windturbine1	2	0	300	1.073	0
Fuel cell	3	30	260	0.294	0.96
Microturbine1	4	25	260	0.457	1.65
Battery	5	−180	180	0.38	0
Microturbine2	6	50	250	0.215	1.65
Microturbine3	7	65	250	0.275	1.65
Windturbine2	8	0	200	1.073	0

recording of the corresponding data are used to train the support vector machine and provide a forecast data. Comparing the forecast signal with the real dataset, one can extract out the standard deviation value for the probability density function of the uncertain parameter as explained in Section 3.

Step 3: Produce a random pollen population in the problem feasible domain. Each pollen is a math vector showing the optimal switching status as well as the optimal output power of DGs, storage and main grid in the hybrid AC/DC microgrid as follows:

$$X_k = [\lambda_{Tie}, \lambda_{Sw}, P_G, U_G, P_S, P_{grid}]_{(M_{Tie}+M_{Sw}+2\times N_g+N_s+1)\times N_T} \quad \forall l \in \Omega^{FP} \tag{37}$$

Step 4: The charging demand of electric vehicles are determined based on the roulette wheel mechanism. Here the charger type, capacity, rate, vehicle market share and battery type are considered as in Section 2 in a random process to provide the expected charging demand in the grid.

Step 5: Run the stochastic framework based on point estimate method in Section 3 to calculate the expected value of the cost function. To this end, the concentration points are calculated as explained in (16)–(18) and then the expected cost value is determined as (19)–(21).

Step 6: The best solution X_g is stored according to the expected cost function value in (22).

Step 7: Update the pollen population based on (31)–(33). Through this process, the pollen population moves to a new position, which might result in more fitting X_g.

Step 8: Update the pollen pollution based on (35)–(36). This will help to improve the pollen position once more to increase the diversity and avoid trapping in local optima.

Step 9: Check the termination criteria domain to see whether the algorithm ought to continue or not. If the algorithm converges, then go to step 11 otherwise returns to step 6.

Step 10: Update the pollination constant parameter as in (34).

Step 11: Finish the optimization and print the results. The optimal switching scheme, the charging pattern of electric vehicles, the optimal output power of DGs, storage units and the main grid are the variables, which their results would be published.

7. Simulation results

In this section, an IEEE test system is used to construct a hybrid AC/DC microgrid and assess the proposed model performance on it. The hybrid AC/DC microgrid is constructed by the join connection of two networks, one AC microgrid, which is the IEEE 33-bus test system (Baran and Wu, 1989) and one DC microgrid borrowed from Baziar and Kavousi-Fard (2013). Fig. 4 shows the structure of the hybrid microgrid including the AC area and the DC area. The voltage level of the system is 12.66 kV as the standard requirement (Baran and Wu, 1989) and the AC and DC grids can exchange power on bus 11 as the gateway. In the AC area of the microgrid, two microturbine and one wind turbine are installed in the grid (as shown in Fig. 6). All other data of the microgrid can be found in Baziar and Kavousi-Fard (2013). In the DC area, there are one battery as the energy storage component, one wind turbine, one fuel cell and one microturbine. The capacity, power offering and cost of switching operation for DGs is provided in Table 3. The main assumptions made in this work are considering a symmetrical three-phase system with non-harmonic loads. In addition, the electrical loads are modeled as constant P–Q model.

Table 4
TIE switches data.

Switch number	Connection		Impedance values (ohm)	
	From bus	To bus	Resistance	Reactance
33	8	21	2	2
34	9	15	2	2
35	12	22	2	2
36	18	33	0.5	0.5
37	25	29	0.5	0.51.0

Figs. 7 and 8 show the utility price and the load factor of the system for 24 h of scheduling. The system is equipped with five remotely control switches as normal open switches and thirty-two normally switches. By the use of these switches, one can decide to alter the grid topology and provide the most optimal structure.

According to the historical data recorded for the electric vehicles, it is expected that there would be around 250 residents with electric vehicles in the area of the hybrid microgrid. Considering the residential type of the microgrid, it is expected that the vehicles are distributed all around the microgrid, which makes it so challenging to run optimal scheduling. Table 4 provides the tie switches information located in the system. The forecast values of the wind units as well as the solar panel are plotted in the same curve as in Fig. 9.

In the first part of the simulations, the search competency of the MFPA is compared to the particle swarm optimization (PSO) (Mohamed et al., 2016) and genetic algorithm (GA) (Mohamed et al., 2015). The simulation results over a hundred iterations for the expected cost function is plotted for all algorithms in Fig. 10. According to these results, the proposed MFPA could converge first in less than 20 iterations much faster than GA and PSO. Moreover, the algorithm could escape from the local optimum, which others have fallen in. These results show the appropriate performance of the algorithm for solving the problem. Therefore, this method is used as the problem solver from now on. To make a deep analysis, the simulations are implemented in three different scenarios including the coordinated charging, uncoordinated charging and smart charging schemes. In addition, two different penetration levels of 40% and 80% are considered to highlight the charging effect of plug in hybrid electric vehicles on the system operation.

In the first scenario, electric vehicles can start charging in an uncoordinated way, i.e. the car owner can plug-in his car to the charger point as he/she gets home. The simulation results for

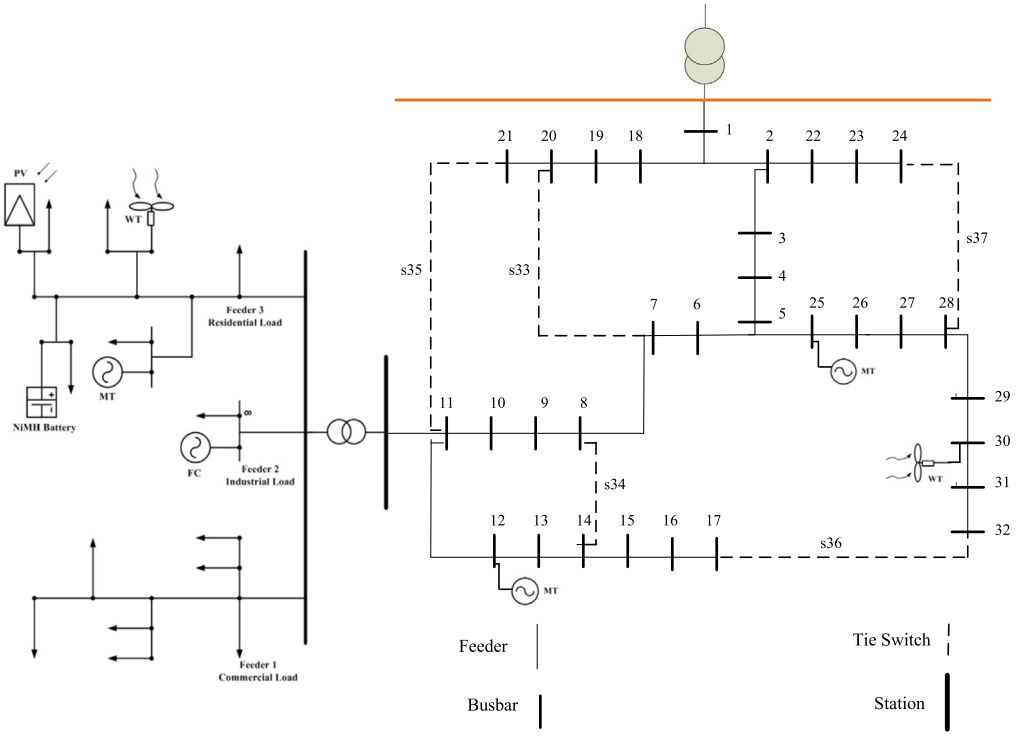

Fig. 6. Single-line diagram of the test microgrid.

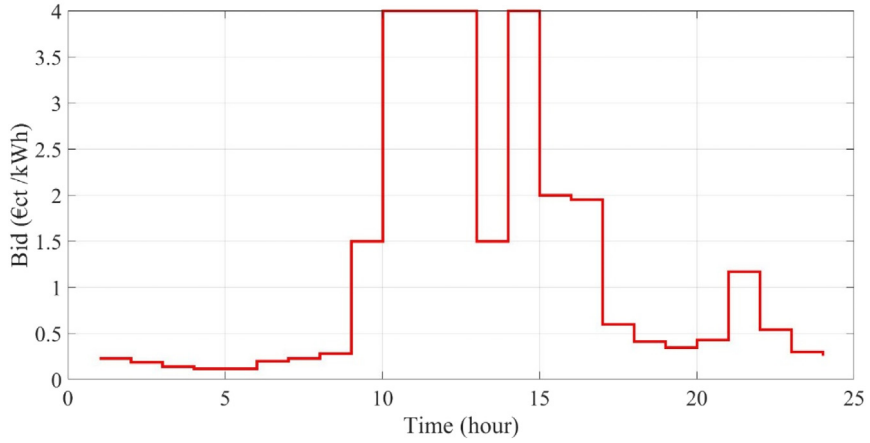

Fig. 7. Market price offered by the main grid.

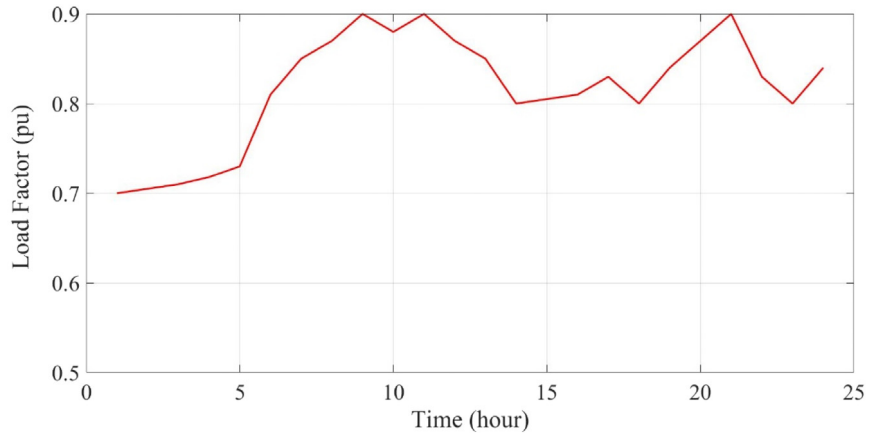

Fig. 8. Load factor for the next day scheduling problem.

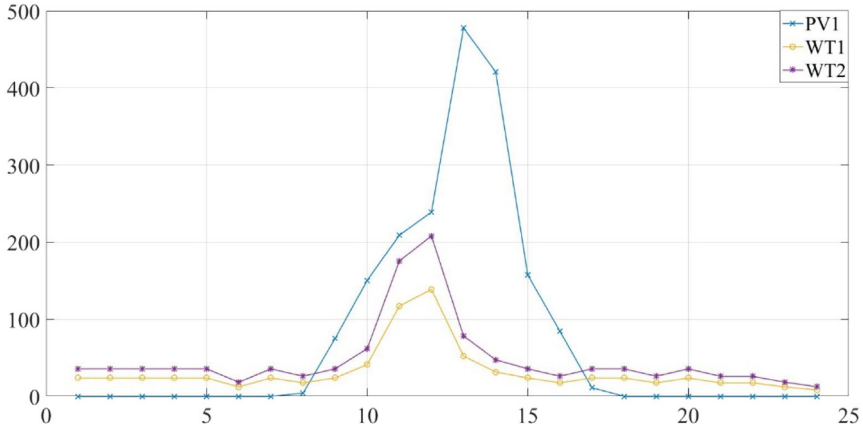

Fig. 9. Hourly generated power of wind units and solar units.

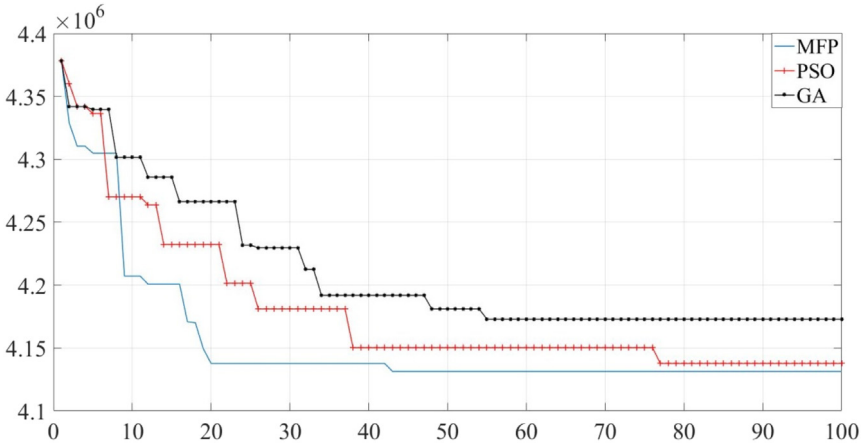

Fig. 10. Convergence characteristics of MFPA, PSO and GA in optimizing the total cost function for 100% penetration of electric vehicles in smart charging.

this scenario are shown in Table 5 considering 40% penetration level. The hourly microgrid cost value before and after optimal switching is shown in the table. According to these results, the microgrid cost has mitigated through the optimal switching. The open switches of the system are shown in the table as well. The optimal output power of DGs and battery are shown in Fig. 11. According to this figure, the battery is charging in the first hours to help reducing the microgrid cost at the peak load hours, i.e. mid-day. Also, it is seen that the wind turbine and the solar unit are producing power as predicted due to the nondispatchable nature of these renewables. It is preferred to purchase less power from the expensive units as long as the price offer is higher that the main grid electricity price.

The second scenario assumes that all electric vehicles are dedicated to the coordinated charging. Table 6 shows the optimal switching scheme along with the cost of the microgrid before and after the switching. By postponing the charging starting time of electric vehicles to off-peak hours, it is seen that the microgrid cost has reduced in most of the hours. Also it is seen that altering the microgrid topology has affected the microgrid cost in a decreasing manner. The optimal operating points of the generators and battery are shown in Fig. 12. Compared to the first scenario, it is seen that the some units are generating lower power at the middle of the day, which is a direct effect of the coordinated charging pattern.

The third scenario is dedicated to the smart charging scheme, wherein the market price and load demand situation are considered in the charging time. Table 7 shows the microgrid cost before and after switching as well as the optimal structure of the grid. According to these results, the microgrid is experiencing less pressure from the charging of electric vehicles in comparison with the last two scenarios. This not only has reduced the hourly cost of the microgrid, but also has changed the grid topology for providing better matching with the units. The optimal output power of units is shown in Fig. 13. Similar discussion with the last figures can be made here. For better comparison, the total cost of the microgrid for all scenarios and for penetration levels of 40% and 80% are provided in Fig. 14. The first direct result of this figure is that a higher penetration level of the electric vehicles appears as additional cost for the hybrid microgrid. Also, it is seen that optimal switching has been useful for improving the microgrid economic situation by proving alternative power flow path and thus reducing the costs. Moreover, the effectiveness and high efficacy of the smart charging pattern compared to the coordinated and uncoordinated patterns can be deduced here. It is seen that the smart charging scheme could reduce the total operation cost of the hybrid microgrid in most of the hours. This is an indirect but positive effect of shifting the charging demand of the electric vehicles to off-peak load hours. From a technical point of view, this can help to avoid feeder congestion and releasing the unused capacity of the units. Moreover, since the microgrid topology is changing actively, this could help for better power dispatch of the wind turbine and power flow. This has reduced the power losses and increased the power balance on the feeders.

It should also be noted that the higher the penetration level, the more complex and harder the optimal power dispatch and switching would be. In other words, a higher penetration level demands more active power from the microgrid, which may affect

Table 5
Optimal switching considering uncontrolled charging strategy (Penetration level = 40%).

Hour	Expected cost function value ($)×$10^5$		Open switches after changing the topology				
	Before optimal switching	After optimal switching					
1	0.8397	0.7380	33	12	8	32	24
2	0.7100	0.6291	33	12	35	15	22
3	0.5847	0.5437	20	34	21	30	37
4	0.5908	0.4407	33	34	35	36	37
5	0.5598	0.4776	20	14	21	36	22
6	0.9568	0.7969	33	14	35	36	37
7	0.9868	0.9437	3	14	35	15	24
8	1.2325	1.1857	33	34	35	17	37
9	2.1916	2.1440	33	12	35	15	37
10	2.5550	2.5281	33	34	11	36	37
11	3.2226	3.2863	33	34	35	16	37
12	1.5272	1.4422	7	34	21	36	24
13	0.4022	0.3490	7	14	8	36	37
14	1.6685	1.6647	33	14	35	15	37
15	3.6451	3.6133	33	34	11	32	24
16	3.6644	3.5777	33	14	35	15	37
17	2.2564	2.1495	33	34	35	32	24
18	2.0739	1.9250	33	34	35	36	37
19	2.1071	1.9956	33	34	21	36	23
20	2.5018	2.3981	33	14	10	36	37
21	3.2158	3.1083	33	14	8	36	37
22	2.8124	2.7067	20	14	8	17	22
23	1.3213	1.2624	20	12	35	36	22
24	1.0673	0.9585	2	12	8	15	37

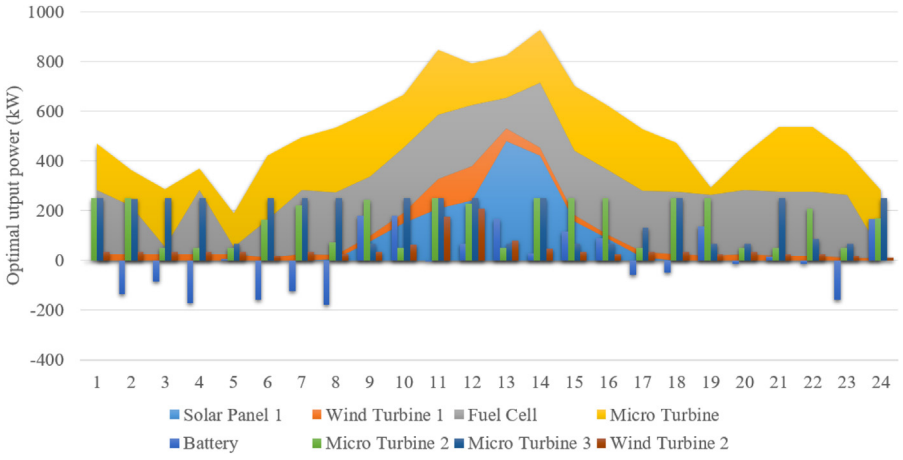

Fig. 11. Optimal power of units uncoordinated charging strategy (Penetration level = 40%).

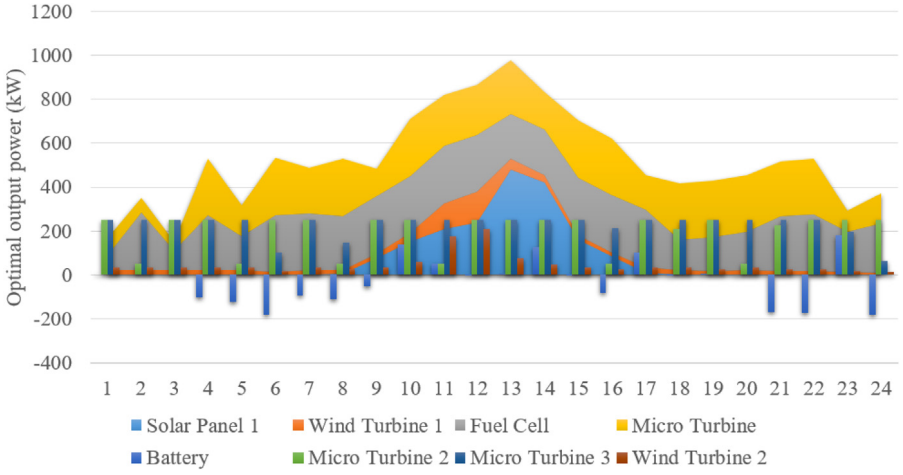

Fig. 12. Optimal power of units in coordinated charging strategy (Penetration level = 40%).

Table 6
Optimal switching considering coordinated charging strategy (Penetration level = 40%).

Hour	Expected cost function value ($)×$10^5$		Open switches after changing the topology				
	Before optimal switching	After Optimal switching					
1	0.6020	0.4756	33	13	11	15	24
2	0.7274	0.6640	20	14	8	32	37
3	0.6140	0.5470	2	34	35	36	24
4	0.4411	0.4000	2	34	21	32	22
5	0.5584	0.5568	2	34	8	36	37
6	0.9151	0.8720	3	14	8	17	37
7	1.0532	1.0147	33	34	21	36	37
8	1.1209	0.9885	33	14	8	15	22
9	2.2004	2.1121	33	34	21	15	37
10	2.5769	2.5517	20	34	35	36	37
11	3.3538	3.2621	33	34	11	32	37
12	1.4962	1.3911	33	34	21	36	37
13	0.4214	0.3453	20	14	35	36	24
14	1.6873	1.6259	33	34	35	32	37
15	3.7077	3.6861	33	34	35	36	37
16	3.5693	3.5156	33	14	11	36	37
17	2.1835	2.1402	33	13	35	32	24
18	1.8888	1.8275	20	34	21	15	37
19	2.0045	1.9232	4	34	35	17	24
20	2.4610	2.4460	33	34	35	17	24
21	3.0054	2.8996	7	34	21	32	22
22	2.7240	2.6303	33	14	21	15	37
23	1.1945	1.0983	2	34	21	36	37
24	1.0466	1.0346	20	34	35	32	22

Table 7
Optimal switching considering coordinated charging strategy (Penetration level = 40%).

Hour	Expected cost function value ($)×$10^5$		Open switches after changing the topology				
	Before optimal switching	After optimal switching					
1	0.5111	0.4582	7	34	21	17	23
2	0.7102	0.6128	7	34	21	36	37
3	0.6056	0.5318	20	12	35	36	37
4	0.3675	0.3034	20	14	21	31	37
5	0.5531	0.5055	33	34	21	36	24
6	0.8555	0.7871	20	34	11	15	24
7	0.9707	0.9543	20	34	21	32	37
8	1.1169	1.0434	33	34	8	32	24
9	2.1328	2.0626	33	13	35	32	37
10	2.5614	2.4634	7	14	8	15	24
11	3.3207	3.2724	20	13	35	36	37
12	1.4958	1.4572	20	12	21	15	37
13	0.3882	0.3877	7	14	21	36	37
14	1.6737	1.6060	33	34	35	17	37
15	3.6633	3.6077	33	34	35	17	37
16	3.5660	3.4825	33	34	21	32	37
17	2.1690	2.1268	33	34	11	31	37
18	1.7901	1.7040	6	34	21	17	24
19	1.9822	1.9365	33	14	35	15	37
20	2.3960	2.3855	7	14	35	36	24
21	2.9166	2.9074	20	34	35	32	24
22	2.6971	2.6120	33	12	35	15	37
23	1.1852	1.1534	33	12	8	36	37
24	0.9768	0.8795	7	34	35	30	22

the entire power dispatch and automation process. In response to this big challenge, a smart charging strategy can mitigate the burden on the grid by distributing the total charging demand at off-peak load hours. Therefore, it is seen that smart charging could help reducing the total operation cost of the hybrid AC–DC microgrid compared to the controlled and uncontrolled charging schemes. From the automation point of view, this has affected the system topology at most of the hours to provide new power flow paths for more economic power supply of the loads. It is clear that this has resulted in less power losses and thus enhanced voltage profile for the microgrid.

8. Conclusion

Hybrid AC/DC microgrid has introduced new advantages and merits to the power grids by omitting the many converting devices of AC–DC and DC–AC. Direct access to the electrical power with the same type not only could diminish the total cost of the microgrid, but could also improve the electrical services to the end consumers. This paper investigates the optimal scheduling and energy management of the hybrid AC/DC microgrids in the bed of a novel stochastic data-driven approach. Being equipped with advanced intelligent methods, estimation solutions, switching the feeders and evolutionary algorithms, the proposed framework is so capable of handling the uncertainties associated with the renewable sources, electric vehicle charging

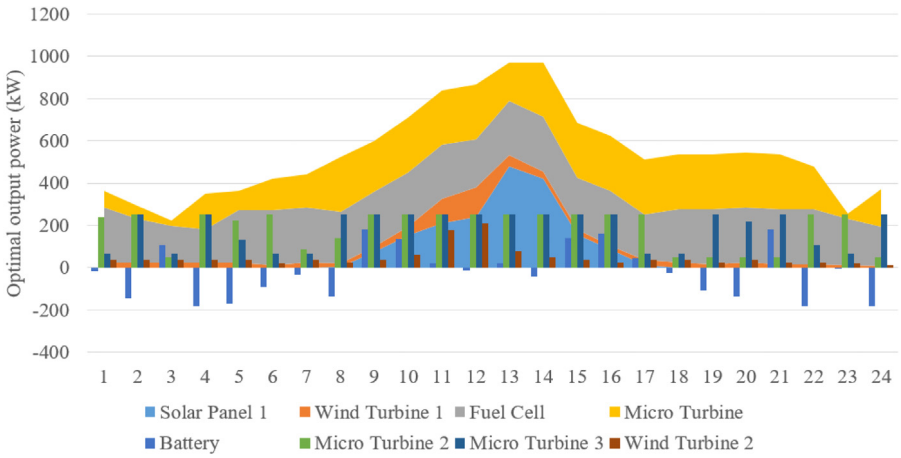

Fig. 13. Optimal power of units in smart charging strategy (Penetration level = 40%).

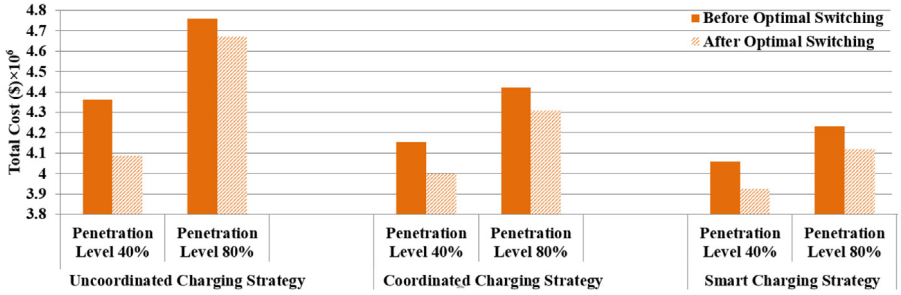

Fig. 14. Effect of plug in hybrid electric vehicle on the total cost of the hybrid AC/DC microgrid.

demand, market price and the consumers load demand. Three different charging schemes, called coordinated, uncoordinated and smart charging was also proposed to assess the different behavior of the car owners and its effects on the microgrid. The simulation results in three different scenarios and two penetration levels of 40% and 80% reveal that optimal switching is always a precious key solution in the operators' hands for reducing the microgrid costs. In addition, it is deduced that a smart charging scheme can help reducing the hourly cost by considering the price and load value factors in the analysis. In terms of the optimization algorithm, the appropriate search characteristics of the proposed MFPA over the GA and PSO as popular benchmarks are assessed.

Therefore, the main advantages of the proposed method can be named as follows:

- Providing a practical stochastic framework which makes it possible to operate the hybrid microgrids incorporating the high uncertainties of the renewable energy sources
- Assessing the charging effect of plug in hybrid electric vehicles on the optimal operation of hybrid microgrids
- Developing a general optimization algorithm, which its stable and reliable performance is not limited only to the microgrids.
- Clarifying the high positive role of switching on the total operation cost of the hybrid microgrids

Along with the above advantages, a few limitations exist which may be addressed in future works. The security of the hybrid microgrids may be affected by the plug in electric vehicles. Therefore, there is a need to a security architecture which can stop hackers from penetrating the microgrid through the electric vehicles. It is needed to assess also other types of electric vehicles such as fuel cell based electric vehicles. For the future works, it is suggested to assess the dynamic aspects of the electric vehicles on the optimal operation of the microgrids. In addition, it is suggested to check other new optimization algorithms to figure out the main pros and cons of the model.

CRediT authorship contribution statement

Peng Wang: Conceptualization, Software, Resources, Visualization. **Dan Wang:** Project administration, Resources, Funding acquisition. **Chengliang Zhu:** Conceptualization, Software, Resources, Visualization. **Yan Yang:** Resources, Software, Validation, Funding acquisition. **Heba M. Abdullah:** Data curation, Resources, Writing - review & editing, Funding acquisition. **Mohamed A. Mohamed:** Conceptualization, Methodology, Software, Validation, Formal analysis, Investigation, Resources, Data curation, Writing - original draft, Writing - review & editing, Visualization, Supervision.

Declaration of competing interest

The authors declare that they have no known competing financial interests or personal relationships that could have appeared to influence the work reported in this paper.

Acknowledgment

This work was supported by the Scientific Research Foundation for Young and Middle-aged of Qinghai University (2019-QGY-12)

References

Aghajani, Gholamreza, Ghadimi, Noradin, 2018. Multi-objective energy management in a micro-grid. Energy Rep. 4, 218–225.

Al-Saud, Mamdooh, Eltamaly, Ali M., Mohamed, Mohamed A., Fard, Abdollah Kavousi, 2020. An intelligent data-driven model to secure intra-vehicle communications based on machine learning. IEEE Trans. Ind. Electron. 67 (6).

Amirkhan, Salman, Radmehr, Masoud, Rezanejad, Mohammad, Khormali, Shahab, 2020. A robust control technique for stable operation of a DC/AC hybrid microgrid under parameters and loads variations. Int. J. Electr. Power Energy Syst. 117, 105659.

Aprilia, Ernauli, Meng, Ke, Al Hosani, Mohamed, Zeineldin, Hatem H., Dong, Zhao Yang, 2019. Unified power flow algorithm for standalone AC/DC hybrid microgrids. IEEE Trans. Smart Grid 10 (1).

Avatefipour, Omid, Al-Sumaiti, Ameena Saad, El-Sherbeeny, Ahmed M., Awwad, Emad Mahrous, Elmeligy, Mohammed A., Mohamed, Mohamed A., Malik, Hafiz, 2019. An intelligent secured framework for cyberattack detection in electric vehicles' CAN bus using machine learning. IEEE Access 7, 127580–127592.

Ayodele, Esan, Misra, Sanjay, Damasevicius, Robertas, Maskeliunas, Rytis, 2019. Hybrid microgrid for microfinance institutions in rural areas – A field demonstration in West Africa. Sustain. Energy Technol. Assess. 35, 89–97.

Balderrama, Sergio, Lombardi, Francesco, Riva, Fabio, Canedo, Walter, Quoilin, Sylvain, 2019. A two-stage linear programming optimization framework for isolated hybrid microgrids in a rural context: The case study of the El Espino community. Energy 1881, 116073.

Baran, M.E., Wu, F.F., 1989. Network reconfiguration in distribution systems for loss reduction and load balancing. IEEE Trans. Power Deliv. 4 (2), 43–57.

Baziar, A., Kavousi-Fard, A., 2013. Considering uncertainty in the optimal energy management of renewable micro-grids including storage devices. Renew. Energy 59, 158–166.

Dabbaghjamanesh, Morteza, Kavousi-Fard, Abdollah, Mehraeen, Shahab, Zhang, Jie, Dong, Zhao Yang, 2020. Sensitivity analysis of renewable energy integration on stochastic energy management of automated reconfigurable hybrid AC–DC microgrid considering DLR security constraint. IEEE Trans. Ind. Inf. 16 (1).

Eghtedarpour, Navid, Farjah, Ebrahim, 2014. Power control and management in a hybrid AC/DC microgrid. IEEE Trans. Smart Grid 5 (3).

Esfahani, Mohammad Mahmoudian, Mohammed, Osama, 2019. Real-time distribution of en-route electric vehicles for optimal operation of unbalanced hybrid AC/DC microgrids. eTransportation 1, 100007.

Ganesan, T., Vasant, P., Sanghvi, P., Thomas, J., Litvinchev, I., 2020. Random matrix generators for optimizing a fuzzy biofuel supply chain system. J. Adv. Eng. Comput. 4 (1).

Ge, Xiaohai, Han, Hua, Xiong, Wenjing, Su, Mei, Sun, Yao, 2020. Locally-distributed and globally-decentralized control for hybrid series-parallel microgrids. Int. J. Electr. Power Energy Syst. 116, 105537.

Gong, Xuan, Dong, Feifei, Mohamed, Mohamed A., Abdalla, Omer M., Ali, Ziad M., 2020. A secured energy management architecture for smart hybrid microgrids considering PEM-fuel cell and electric vehicles. IEEE Access.

Guo, Hongqiang, Wang, Xiangyu, Li, Liang, 2019. State-of-charge-constraint-based energy management strategy of plug-in hybrid electric vehicle with bus route. Energy Convers. Manage. 1991, 111972.

Kavousi-Fard, A., Niknam, T., 2015. Multi-objective stochastic distribution feeder reconfiguration from the reliability point of view. Energy 64, 342–354.

Kavousi-Fard, A., Samet, H., Marzbani, F., A new hybrid modified firefly algorithm and support vector regression model for accurate short term load forecasting. Expert Syst. Appl. 41 (13) 6047–6056.

Li, G., Zhang, X.-P., 2012. Modeling of plug-in hybrid electric vehicle charging demand in probabilistic power flow calculations. IEEE Trans. Smart Grid 3 (1), 492–499.

Mohamed, M.A., Awwad, E.M., El-Sherbeeny, A.M., Nasr, E.A., Ali, Z.M., 2020a. Optimal scheduling of reconfigurable grids considering dynamic line rating constraint. IET Gener. Transm. Distrib. 14 (10), 1862–1871.

Mohamed, M.A., Eltamaly, A.M., Alolah, A.I., 2015. Sizing and techno-economic analysis of stand-alone hybrid photovoltaic/wind/diesel/battery power generation systems. J. Renew. Sustain. Energy 7 (6), 063128.

Mohamed, M.A., Eltamaly, A.M., Alolah, A.I., 2016. PSO-based smart grid application for sizing and optimization of hybrid renewable energy systems. PLoS One 11 (8), e0159702.

Mohamed, Mohamed A., Tajik, Elham, Awwad, Emad Mahrous, El-Sherbeeny, Ahmed M., Elmeligy, Mohammed A., Ali, Ziad M., 2020b. A two-stage stochastic framework for effective management of multiple energy carriers. Energy 197, 117170.

Naderi, M., Bahramara, S., Khayat, Y., Bevrani, Hassan, 2017. Optimal planning in a developing industrial microgrid with sensitive loads. Energy Rep. 3, 124–134.

Peesapati, Rajagopal, Yadav, Vinod Kumar, Kumar, Niranjan, 2018. Flower pollination algorithm based multi-objective congestion management considering optimal capacities of distributed generations. Energy 14715, 980–994.

Pourbehzadi, Motahareh, Niknam, Taher, Aghaei, Jamshid, Mokryani, Geev, Catalão, João P.S., 2019. Optimal operation of hybrid AC/DC microgrids under uncertainty of renewable energy resources: A comprehensive review. Int. J. Electr. Power Energy Syst. 109, 139–159.

Ray, Prakash K., Mohanty, Asit, 2019. A robust firefly–swarm hybrid optimization for frequency control in wind/PV/FC based microgrid. Appl. Soft Comput. 85, 105823.

Roustaei, M., Niknam, T., Salari, S., Chabok, H., Sheikh, M., Kavousi-Fard, A., A scenario-based approach for the design of smart energy and water hub. Energy 116931.

Shao, Minglei, Wang, Xin, Bu, Zhen, Chen, Xiaobo, Wang, Yuqing, 2020. Prediction of energy consumption in hotel buildings via support vector machines. Sustainable Cities Soc. 57, 102128.

Sur, Ujjal, Biswas, Amitava, Bera, Jitendra Nath, Sarkar, Gautam, 2020. A modified holomorphic embedding method based hybrid AC-DC microgrid load flow. Electr. Power Syst. Res. 182, 106267.

Tabar, Vahid Sohrabi, Ghassemzadeh, Saeid, Tohidi, Sajjad, 2019. Energy management in hybrid microgrid with considering multiple power market and real time demand response. Energy 1741, 10–23.

Vasant, P., Zelinka, I., Weber, G.W., 2019a. Intelligent computing & optimization. Adv. Intell. Syst. Comput..

Vasant, P., Zelinka, I., Weber, G.W., 2019b. Intelligent computing and optimization. In: Proceedings of the 2nd International Conference on Intelligent Computing and Optimization 2019 (ICO 2019).

Wang, Chengshan, Li, Xialin, Guo, Li, Li, Yun Wei, 2014. A nonlinear-disturbance-observer-based DC-bus voltage control for a hybrid AC/DC microgrid. IEEE Trans. Power Electron. 29 (11).